*ECS Electrochemistry Letters*, **4** (3) A33-A36 (2015)
2162-8726/2015/4(3)/A33/4/$31.00 © The Electrochemical Society


# Preparation of Mesoporous Si@PAN Electrodes for Li-Ion Batteries via the In-Situ Polymerization of PAN

**Thomas A. Yersak,[a,*] JaeWook Shin,[a] Ziying Wang,[a] Daniel Estrada,[b] Justin Whiteley,[c] Se-Hee Lee,[c,*] Michael J. Sailor,[b,*] and Ying Shirley Meng[a,*,z]**

[a]*Department of Nano Engineering, University of California San Diego, La Jolla, California 92093-0448, USA*
[b]*Department of Chemistry and Biochemistry, University of California San Diego, La Jolla, California 92093-0358, USA*
[c]*Department of Mechanical Engineering, University of Colorado Boulder, Boulder, Colorado 80309-0427, USA*

This paper details a new binder for mesoporous Si (mp-Si) via the in-situ polymerization and stabilization of polyacrylonitrile (PAN). Using this method mp-Si@PAN electrodes for Li-ion battery anodes have been fabricated. Though the mp-Si@PAN electrodes delivered a reversible specific capacity in excess of 800 mAh $g^{-1}$ (electrode), the first cycle coulombic efficiency of these electrodes was still less than 50% without a pre-lithiation treatment. The results of an all-solid-state battery experiment confirmed that low first cycle reversibility should be attributed primarily to mechanical pulverization of the internal porous structure of mp-Si particles.
 [DOI: 10.1149/2.0011503eel] 

Manuscript received December 12, 2014. Published January 9, 2015.

Many porous Si nanostructured anode materials have been proposed for advanced Li-ion batteries.[1–7] A recent study utilizing 5–10 μm diameter mesoporous Si (mp-Si) particles demonstrates that strain accommodation by pore volume can limit the bulk expansion of mp-Si particles to 30%.[8] Composite electrodes made with these mp-Si particles deliver a specific capacity of approximately 750 mAh $g^{-1}$ (electrode) after 800 cycles. Such a stable performance is attributed to preservation of the composite electrode structure. Unfortunately, these electrodes require a pre-lithiation treatment in order to offset a large first cycle irreversibility (> 40%). It is not clear whether the large irreversibility is due to the formation of a solid electrolyte interphase (SEI) on mp-Si's large surface area or the mechanical pulverization of the internal porous structure.

To investigate how to improve mp-Si's reversibility, this study utilizes a stabilized polyacrylonitrile (PAN) conductive binder. Stabilized PAN has been demonstrated as a conductive binder for both nano-Si[9,10] and macroporous Si[6] electrodes. The stabilization process dehydrogenates and cyclizes PAN so as to impart the structure with delocalized $sp^2$ π bonding for intrinsic electronic conductivity but avoids full carbonization to retain polymeric elasticity.[11,12] Macromolecules of PAN (Mw = 150,000 g $mol^{-1}$) can infiltrate macropores, however, macromolecules cannot infiltrate mesopores. For this reason, we propose the in-situ polymerization and stabilization of PAN where an acrylonitrile (AN) monomer solution infiltrates Si mesopores. The PAN binder adheres to both the internal porous structure and the external bulk of the micron-sized mp-Si particles so as to produce a mp-Si@PAN electrode. Figure 1 schematically compares the structure of the mp-Si@PAN electrode with that of a conventional mp-Si bulk PAN electrode. The work presented here represents the first demonstration of mp-Si carbonization with stabilized PAN.

It will be shown that a PAN binder does not influence the reversibility of mp-Si's first electrochemical cycle. An all-solid-state battery architecture can be used to probe the lithiation mechanisms of Si.[13] Here we adopt a similar strategy in order to better understand mp-Si's first cycle irreversibility as mechanical or chemical in nature. All-solid-state composite electrodes utilize a glass electrolyte and have limited interfacial contact so that losses due to electrolyte decomposition are minimized. It is found that an all-solid-state battery does not improve mp-Si's first cycle coulombic efficiency (CE) and that first cycle losses should be attributed primarily to pulverization of the delicate internal porous structure.

## Methods and Materials

All electrode slurry preparation and test cell construction was conducted in a dry Ar glove box (MBraun UniLab). The mp-Si particles shown in Figure 1 were synthesized as described elsewhere.[8] The conventional "mp-Si bulk PAN" electrode was prepared as described previously with PAN (Sigma Aldrich, Mw = 150,000 g $mol^{-1}$) and a mp-Si:PAN weight ratio of 6:4.[9] The mp-Si bulk PAN electrode Si mass loading was 0.29 mg $cm^{-2}$. The preparation of the "mp-Si@PAN" electrodes first required combining 10 mL of *N,N*-dimethylformamide (DMF, Sigma Aldrich), 9.86 mg of azobisisobutyronitrile salt (AIBN, Sigma Aldrich), and 3 mL of acrylonitrile (AN, Sigma Aldrich). Next, 50 mg of mp-Si and 540 μL of the aforementioned solution were combined in a 4 mL vial with a magnetic stir bar. This mixture was stirred for 12 hours at 20°C and for a further 24 hours at 70°C. Prior to blading, 100 μL of DMF was added to the slurry to decrease its viscosity. The electrode was bladed (8 mil) onto copper foil (Alfa Aesar), dried, calendared, and stabilized in a tube furnace with constant dry Ar gas flow at 300°C for 12 hours. The mp-Si@PAN electrode Si mass loading was 0.58 mg $cm^{-2}$.

Raman spectroscopic data was collected on a Renishaw inVia microRaman equipped with a 488 nm laser. A focus ion beam (FIB) equipped scanning electron microscope (FIB/SEM FEI 3D Quanta dualbeam) was used to conduct energy dispersive X-ray spectroscopy (EDS) elemental mapping of cross-sectioned mp-Si particles. mp-Si@PAN powder for Brunauer-Emmett-Teller (BET) surface area was collected by scraping prepared electrodes (Micromeritics ASAP 2010). Electrochemical half cells were assembled using 2032 coin cells, polymer separators (Celgard), 1 mm thick lithium foil, and 1:1 (wt.) EC:DEC (ethylene carbonate:diethyl carbonate) 1 M $LiPF_6$ electrolyte (BASF). Half-cells were cycled with CCCV parameters (0.05 V–1.5 V vs. Li) at 20°C and a C/30 rate for the first cycle and a C/15 rate for all subsequent cycles.

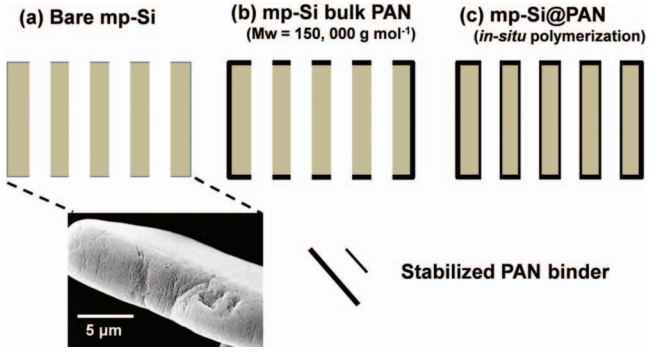


**Figure 1.** Not to scale schematic representations of the mp-Si samples under consideration. Pores are 50 nm in diameter and pore walls are 10 nm thick; both are oriented vertically. Stabilized PAN is represented by black lines.

*Electrochemical Society Active Member.
zE-mail: shirleymeng@ucsd.edu

The mp-Si tested with an all-solid-state battery was carbonized with 20 wt% acetylene.[8] The all-solid-state mp-Si composite electrode was a 3:7 weight ratio of carbonized mp-Si and $77.5Li_2S \cdot 22.5P_2S_5$ glass electrolyte. The all-solid-state battery consisted of a 3 mg composite electrode, a 150 mg glass electrolyte separator and a lithium foil counter electrode.[13] The all-solid-state cells were cycled with CCCV parameters (0.05 V–1.5 V vs. Li) at 60°C and a current density of 50 μA $cm^{-2}$ (C/40) for cycles 1–3 and 100 μA $cm^{-2}$ (C/20) for all subsequent cycles.

## Results and Discussion

The yield of PAN's radical initiated solution polymerization was measured to be 39% in the absence of Si particles. Using this number the Si active mass loading of the mp-Si@PAN electrode was calculated to be 56 wt%. Determining the electrode composition in this way has been described previously.[14]

Raman spectroscopy (Figure 2a) of a mp-Si@PAN electrode was used to confirm the appropriate pyridinic structure for stabilized PAN.

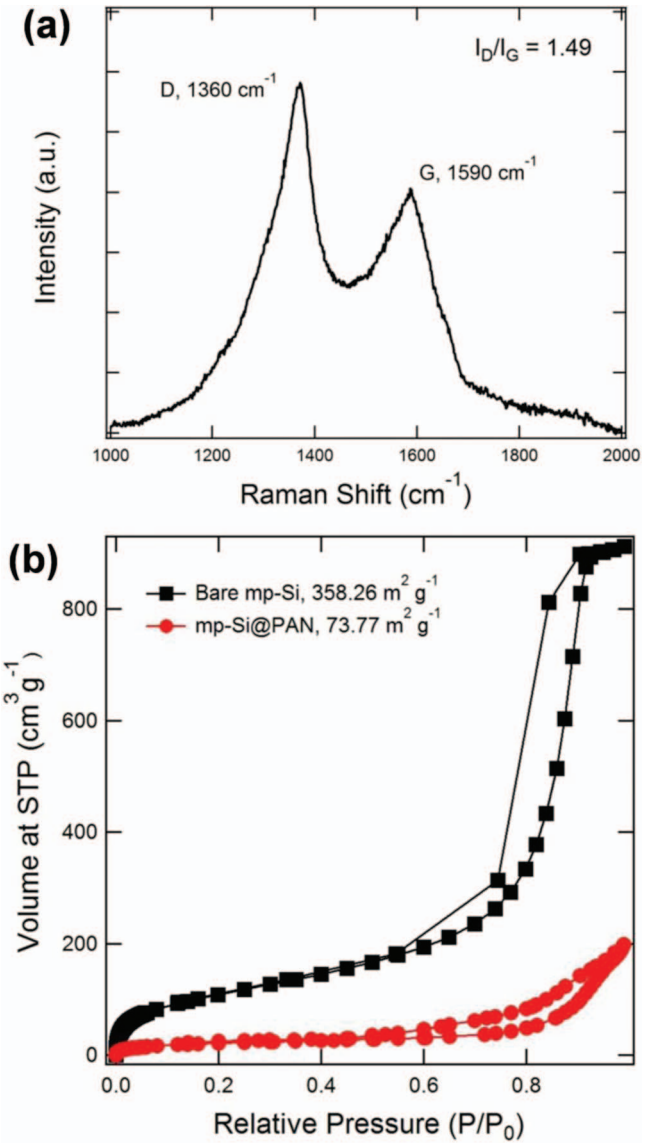


**Figure 2.** (a) Raman spectrum of a mp-Si@PAN electrode surface with 488 nm laser excitation and linear baseline subtraction. (b) BET surface area isotherms of bare mp-Si (black square) and mp-Si@PAN (red circle) powders.

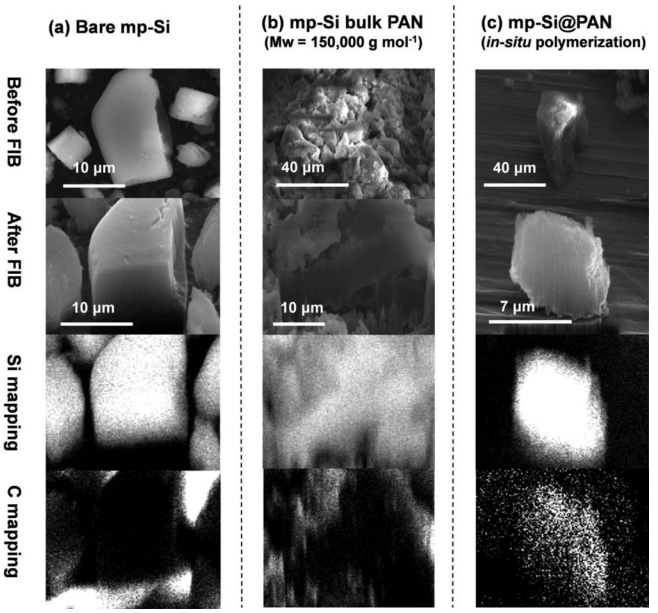


**Figure 3.** Results of FIB cross-sectioning and EDS mapping of (a) bare mp-Si, (b) conventional mp-Si bulk PAN electrode, and (c) mp-Si@PAN electrode. Carbon signals are mapped only to the interior of cross-sectioned mp-Si@PAN electrode particles.

The presence of carbon D (1360 $cm^{-1}$) and G (1590 $cm^{-1}$) bands confirms an intrinsic electronic conductivity by the presence of delocalized $sp^2$ π bonding. Graphite has a $I_D/I_G$ peak ratio of 0.09 whereas a previously described stabilized PAN binder for nano-Si has a $I_D/I_G$ peak ratio of 2.5.[9] As desired, the polymerized and stabilized PAN presented here has a $I_D/I_G$ peak ratio of 1.49 confirming that the material is highly disordered and not highly carbonized.

BET surface area was measured to understand the degree to which PAN filled mp-Si's porous volume. The BET isotherms for bare mp-Si and mp-Si@PAN electrode powder are provided in Figure 2b. Bare mp-Si's BET surface area was 358.26 $m^2$ $g^{-1}$ while the mp-Si@PAN electrode's BET surface area was 73.77 $m^2$ $g^{-1}$. The decrease in BET surface area confirmed that material was deposited within mp-Si.

To confirm that the in-situ polymerization and stabilization of PAN was successful, PAN was directly observed inside mp-Si particles. The results of FIB mp-Si particle cross sectioning and EDS elemental mapping are provided in Figure 3. Three samples were cross-sectioned and mapped: a bare mp-Si particle, a mp-Si particle from the conventional mp-Si bulk PAN electrode, and a mp-Si particle from the mp-Si@PAN electrode. SEM images are provided before and after FIB cross-sectioning. Elemental mapping was conducted after particle cross-sectioning and white contrast represents the presence of an element of interest. As expected, no carbon was mapped to the interior of the bare particle or the particle from the conventional mp-Si bulk PAN electrode. With this observation it was confirmed that macromolecules of PAN (150,000 g $mol^{-1}$) cannot infiltrate mp-Si and that the DMF solvent used in electrode slurry preparation does not leave C residue. C was only mapped to the interior of particles from the mp-Si@PAN electrode. Because AN volatilizes during electrode drying, PAN is the only reasonable source of C. Therefore, it is confirmed that PAN was successfully polymerized and stabilized in-situ. This represents the very first carbonization of mp-Si with PAN.

Electrochemical characterization of the conventional mp-Si bulk PAN electrode and the mp-Si@PAN electrode are provided in Figure 4. The first cycle voltage profiles given in Figure 4a both exhibit plateaus at 0.5 V which are attributed to the reduction of $SiO_x$.[15] Both electrodes delivered a first cycle lithiation specific

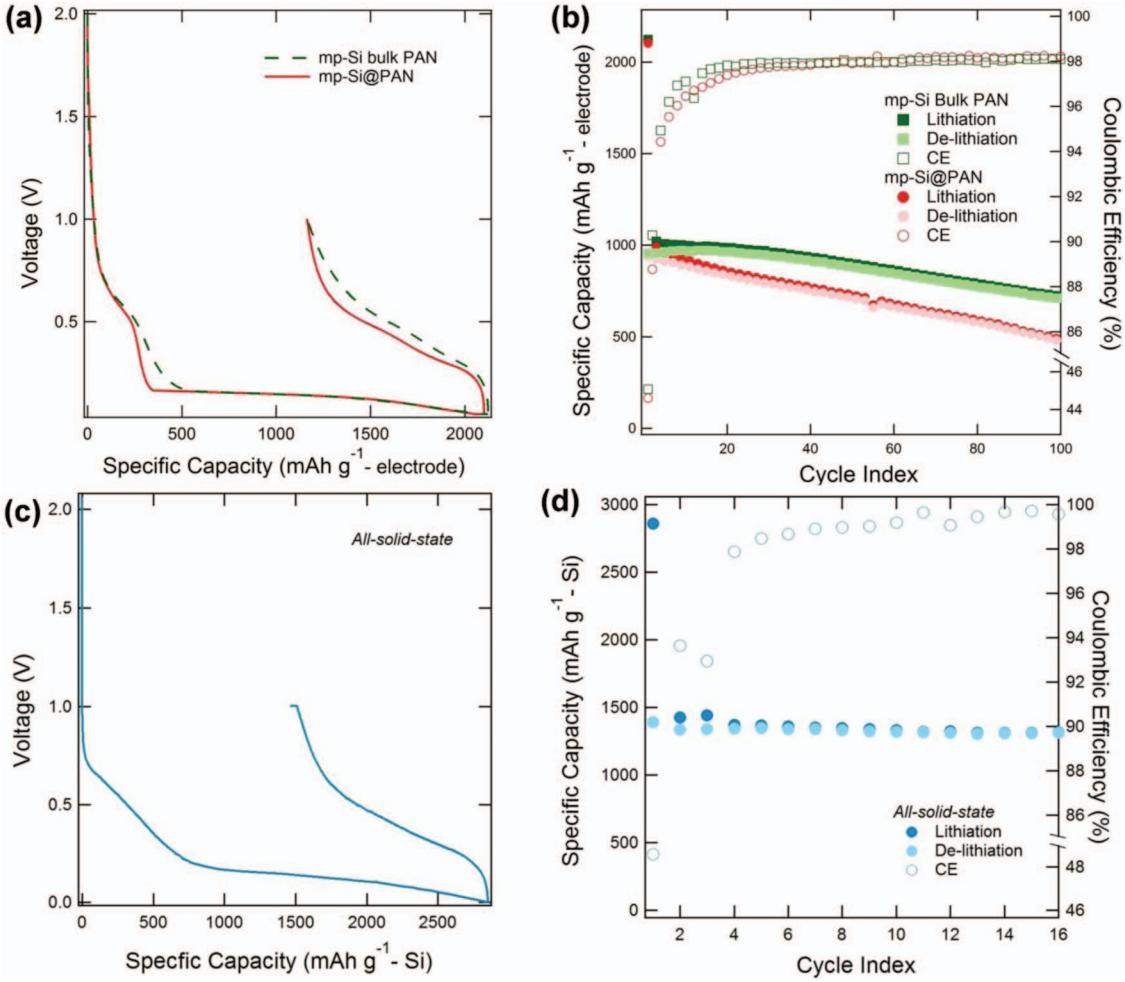


**Figure 4.** (a) First voltage profile for a conventional mp-Si bulk PAN electrode (green) and a mp-Si@PAN electrode (red). (b) Specific capacity and CE for mp-Si electrodes studied in 1:1 (wt.) EC:DEC 1 M $LiPF_6$ electrolyte. (c) First cycle voltage profile for an all-solid-state mp-Si battery (blue). (d) Specific capacity and CE for all-solid-state mp-Si battery with $77.5Li_2S \cdot 22.5P_2S_5$ glass electrolyte. Note: specific capacity accounting for the all-solid-state battery only takes active material mass into account.

capacity of approximately 2100 mAh $g^{-1}$ (electrode) and a first cycle CE of 45%. After 40 cycles, the CE for both electrodes stabilized at 98% (Figure 4b). By the 100$^{th}$ cycle the mp-Si@PAN electrode delivered 490 mAh $g^{-1}$ while the conventional mp-Si bulk PAN electrode delivered 724 mAh $g^{-1}$. The better capacity retention of the conventional mp-Si bulk PAN electrode compared to that of the mp-Si@PAN electrode can be explained by a higher mp-Si:PAN weight ratio (6:4 versus 56:44) and a lower electrode Si mass loading (0.29 mg $cm^{-2}$ versus 0.58 mg $cm^{-2}$).

The comparable electrochemical performance of the conventional mp-Si bulk PAN and the mp-Si@PAN electrodes confirms that the processing of PAN binders can be altered with minimal effect on electrode electrochemistry. Further, the first cycle CE of the mp-Si@PAN electrode was no better than that reported previously.[8] The results of a mp-Si all-solid-state battery are provided in Figure 4c and Figure 4d. The first cycle CE of the mp-Si all-solid-state battery was 48.6%, which is only a small improvement. More impressively, the all-solid-state battery's CE rapidly increased to 99.5% by the 11$^{th}$ cycle. Failure to significantly improve the first cycle CE of mp-Si using an all-solid-state battery indicates that the internal porous structure of mp-Si undergoes catastrophic mechanical pulverization during the first cycle. It is has been suggested that upon delithiation sections of mp-Si's pulverized internal structure become electrically isolated and electrochemically inactive. The internal PAN binder of the mp-Si@PAN electrode is not sufficient to maintain the electrical contact of such a delicate structure.

## Conclusions

In this study we demonstrated the processing versatility of PAN binders. To better understand why the first cycle CE of mp-Si@PAN electrolyte was below 50%, an all-solid-state battery was used to isolate mp-Si's mechanical losses from its electrochemical instability with liquid electrolyte. We found that the first cycle CE of an all-solid-state mp-Si electrode was also below 50%. We conclude that improvement of mp-Si electrodes should focus on a structural optimization of the porous active material in addition to advanced binder processing techniques.

## Acknowledgments

Funding for this study at UCSD was provided by a grant from the U.S. Department of Energy's Office of Vehicle Technologies, Contract No. DE-AC02-05CH11231, Subcontract No. 7056412 under the Batteries for Advanced Transportation Technologies (BATT) Program and a California Institute for Energy and Environment (CIEE) subaward No. PODR05-S16 from the Multiple Campus Award program of the California Energy Commission. Funding for the all-solid-state work at the University of Colorado Boulder was provided by a grant from the National Science Foundation, Contract No. CHE-1231048. Special thanks to Brandon Marin and Prof. Andrea Tao (UCSD) for collecting Raman spectroscopy data and to David Roberts for collecting BET data.

## References


1. R. Yi, F. Dai, M. L. Gordin, H. Sohn, and D. Wang, *Advanced Energy Materials*, **3**, 1507 (2013).
2. R. Yi, F. Dai, M. L. Gordin, S. Chen, and D. Wang, *Advanced Energy Materials*, **3**, 295 (2012).
3. B. M. Bang, J. I. Lee, H. Kim, J. Cho, and S. Park, *Advanced Energy Materials*, **2**, 878 (2012).
4. B. M. Bang, H. Kim, H.-K. Song, J. Cho, and S. Park, *Energy & Environmental Science*, **4**, 5013 (2011).
5. H. Kim, B. Han, J. Choo, and J. Cho, *Angewandte Chemie*, **120**, 10305 (2008).
6. M. Thakur, S. L. Sinsabaugh, M. J. Isaacson, M. S. Wong, and S. L. Biswal, *Scientific reports* **2** (2012).
7. H. Cheng, R. Xiao, H. Bian, Z. Li, Y. Zhan, C. K. Tsang, C. Y. Chung, Z. Lu, and Y. Y. Li, *Materials Chemistry and Physics*, **144**, 25 (2014).
8. X. Li, M. Gu, S. Hu, R. Kennard, P. Yan, X. Chen, C. Wang, M. J. Sailor, J.-G. Zhang, and J. Liu, *Nature Communications*, **5**, 4105 (2014).
9. D. M. Piper, T. A. Yersak, S.-B. Son, S. C. Kim, C. S. Kang, K. H. Oh, C. Ban, A. C. Dillon, and S.-H. Lee, *Advanced Energy Materials*, **3**, 697 (2013).
10. D. M. Piper, J. H. Woo, S.-B. Son, S. C. Kim, K. H. Oh, and S.-H. Lee, *Advanced Materials*, **26**, 3520 (2014).
11. S. K. Nataraj, K. S. Yang, and T. M. Aminabhavi, *Progress in Polymer Science*, **37**, 487 (2012).
12. M. S. A. Rahaman, A. F. Ismail, and A. Mustafa, *Polymer Degradation and Stability*, **92**, 1421 (2007).
13. D. M. Piper, T. A. Yersak, and S.-H. Lee, *Journal of The Electrochemical Society*, **160**, A77 (2013).
14. H. Wu, G. Yu, L. Pan, N. Liu, M. T. McDowell, Z. Bao, and Y. Cui, *Nature Communications*, **4** (2013).
15. K. W. Schroder, H. Celio, L. J. Webb, and K. J. Stevenson, *The Journal of Physical Chemistry C*, **116**, 19737 (2012).